A major purpose of the Technical Information Center is to provide the broadest dissemination possible of information contained in DOE's Research and Development Reports to business, industry, the academic community, and federal, state and local governments.

Although a small portion of this report is not reproducible, it is being made available to expedite the availability of information on the research discussed herein.

Los Alamos National Laboratory is operated by the University of California for the United States Department of Energy under contract W-7405-ENG-36

CONF-8410142--23

LA-UR--84-3316

DE85 002380

TITLE: TRAC-PF1/MOD1 ASSESSMENT AT LOS ALAMOS

AUTHOR(S): Thad D. Knight

SUBMITTED TO: Twelfth Water Reactor Safety Research Information Meeting, National Bureau of Standards, sponsored by the US NRC, Gaithersburg, Maryland, October 22-26, 1984

DISCLAIMER

Los Alamos Los Alamos National Laboratory
Los Alamos, New Mexico 87545

TRAC-PF1/MOD1 ASSESSMENT AT LOS ALAMOS*

by

Thad D. Knight
Safety Code Development Group
Energy Division
Los Alamos National Laboratory
Los Alamos, New Mexico 87545

The Los Alamos National Laboratory is developing the Transient Reactor Analysis Code (TRAC) to provide an advanced best-estimate predictive capability for the analysis of postulated accidents in pressurized water reactors (PWRs). Over the past several years, four distinct versions of the code have been released; each new version introduced improvements to the existing models and numerics and added new models to extend the applications of the code. The first goal of the code was to analyze large-break loss-of-coolant accidents (LOCAs), and the TRAC-P1A and TRAC-PD2 codes[1,2] primarily addressed the large-break LOCA. (The TRAC-PD2/MOD1 code is essentially the same as the TRAC-PD2 code but it also includes a released set of error corrections.) The TRAC-PF1 code[3] contained major changes to the models and trips and to the numerical methods. These modifications enhanced the computational speed of the code and improved the application to small-break LOCAs. The TRAC-PF1/MOD1 code,[4] the latest released version, added improved steam-generator modeling, a turbine component, and a control system together with modified constitutive relations to model the balance of plant on the secondary side and to extend the applications to non-LOCA transients. The TRAC-PF1/MOD1 code also contains reasonably general reactor-kinetics modeling to facilitate the simulation of transients with delayed scram or without scram.

As a part of the code-development process, Los Alamos also conducts developmental assessment of the code before public release. References 5-8 describe the formal developmental assessment for each of the four publicly released code versions. We perform developmental assessment during the later stages of the development process to determine a range of validity for a particular code version, to demonstrate the modeling and calculational capability of the code, and to assist in the setting of empirical constants contained in the constitutive relations in the code. The analyses described in Refs. 5-8 were performed with the final, released code versions.

Independent assessment of a particular code version begins when the code is released. The code version is frozen with the exception that we permit correction of coding errors and updates to improve the handling of boundary conditions as necessary. The purposes of independent assessment are essentially the same as those for developmental assessment except that we change the empirical constants only in sensitivity analyses to investigate discrepancies between the calculated results and the data. The findings of the independent assessment are transmitted to the code developers to aid in

* This work was funded by the USNRC Office of Nuclear Regulatory Research, Division of Accident Evaluation.

correcting errors in the current released code version and to improve the modeling in future code versions.

In the sense that independent assessment involves only released versions of the code and because the results reported in the developmental assessment reports[5-8] were obtained with the final, released versions of the codes, these references constitute the initial independent assessment of the various code versions. The formal independent assessment[9] of the TRAC-P1A code investigated the behavior of that code in a variety of separate-effects and integral tests important to the large-break-LOCA calculational capability. Reference 10 describes the independent assessment of the TRAC-PD2 code (including the TRAC-PD2/MOD1 version); this independent assessment investigated the effects of code improvements on the large-break LOCA capability and extended the applications of the code to small-break LOCAs.

As indicated previously, the TRAC-PF1 code contained many improvements to enhance the application of the code to small-break LOCAs. The developmental assessment mainly investigated the application of the code to small-break LOCAs and tested the new one-dimensional modeling capability. Only a single analysis tied the code back to the large-break LOCA capability in the TRAC-PD2 code that had been tested thoroughly. The independent assessment[11] of TRAC-PF1 provided more testing of the small-break LOCA and began the applications of the code to non-LOCA transient tests.

During the past year, we have completed our independent assessment of the TRAC-PF1 code and begun the independent assessment of the TRAC-PF1/MOD1 code. For the independent assessment of the TRAC-PF1/MOD1 code, we are using several experiments from the Loss-of-Fluid Test (LOFT) and the Semiscale facilities. We also are participating in the International Standard Problem 18 exercise, a Loop Blowdown Investigations (LOBI) small-break LOCA test (for which data currently are unavailable). The developmental assessment[8] of TRAC-PF1/MOD1 consists of analyses of small-break LOCA and natural-circulation tests in the Semiscale Mod-2A facility and non-LOCA transients in the LOFT facility. The independent assessment supports applications of the code to large- and small-break LOCAs and non-LOCA transients and, thus, aids in the resolution of current licensing issues.

We have tested the small-break LOCA capability of TRAC-PF1/MOD1 by analyzing Semiscale Test S-UT-8 (Ref 12). This test simulated a 5% cold-leg break with reduced leakage flow between the cold-leg and hot-leg sides of the system. The test results indicate that the core liquid level drops to the bottom of the core, significantly below the minimum elevation in the pump-suction piping, before the loop seals clear; the extent of the core dryout is enhanced by the formation of liquid levels in the steam-generator tubes on the primary side.

We used a one-dimensional representation of the Semiscale system in our analysis because of the large length-to-diameter ratios throughout the entire system and because of the enhanced calculational speed of the one-dimensional modeling over the three-dimensional modeling (which is only applicable to the pressure vessel). The input model consists of 45 TRAC components, which are subdivided into a total of 198 hydrodynamic cells. Although there are small timing differences between the TRAC-PF1/MOD1 analysis and the data, the code

correctly predicts the phenomena driving the core dryout and the extent of that dryout. Figure 1 compares the calculated and measured upper-plenum pressures. This comparison is quite good. The code correctly represented the effect of the increased pressurizer surge-line resistance that permitted the primary system to decouple from the hot fluid in the pressurizer and to saturate at ~11 MPa initially. The calculated depressurization continues in good agreement with the data until ~360 s, at which time the code begins to underpredict the data slightly. At ~550 s, the calculated rate of depressurization decreased abruptly as liquid from the accumulators reached the core and vapor generation increased. This change in the course of the transient is not reflected in the data.

Figure 2 shows the calculated and measured collapsed liquid levels in the core. The discrepancy between the two liquid levels during the first 100 s is due to flow effects in the measurement and to a difference in the draining of the upper head as shown in Fig. 3. The difference in the draining of the upper head also may impact the comparison as the core drains after 100 s, resulting in a timing offset when the minimum core inventory is reached and in the fact that the data indicate that the level drops below the bottom of the core whereas the calculated minimum level is ~3 cm. Figure 4, a comparison of fluid densities just below the bottom of the core, clearly shows that the difference in minimum core levels is real; the data indicate that shortly after 200 s the liquid drops below this measurement location, but the calculation continues to indicate only liquid during this time. Clearing of

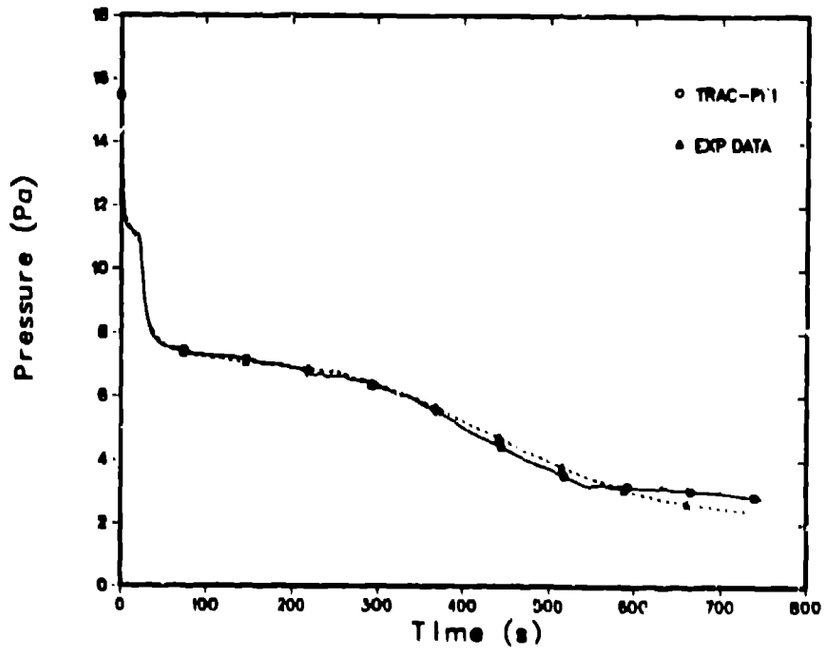

Fig. 1.
Comparison of the TRAC-calculated and measured upper-plenum pressures for Semiscale Test S-UT-8.

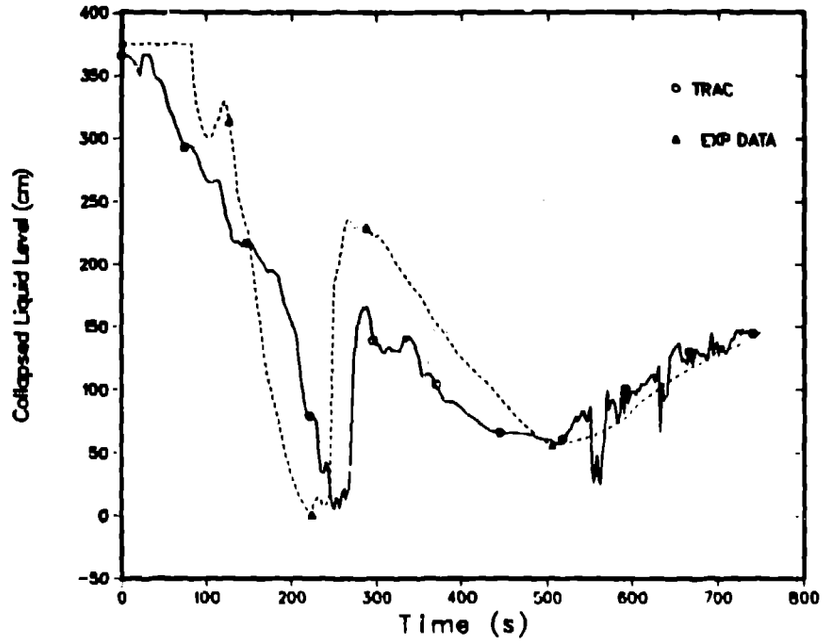

Fig. 2.
Comparison of the TRAC-calculated and measured core collapsed liquid levels for Semiscale Test S-UT-8.

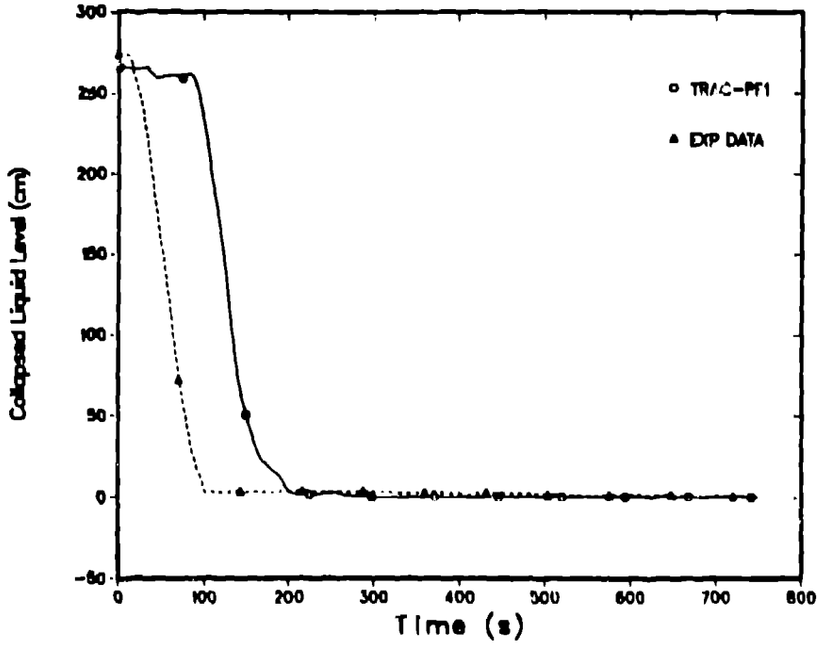

Fig. 3.
Comparison of the TRAC-calculated and measured upper-head collapsed liquid levels for Semiscale Test S-UT-8.

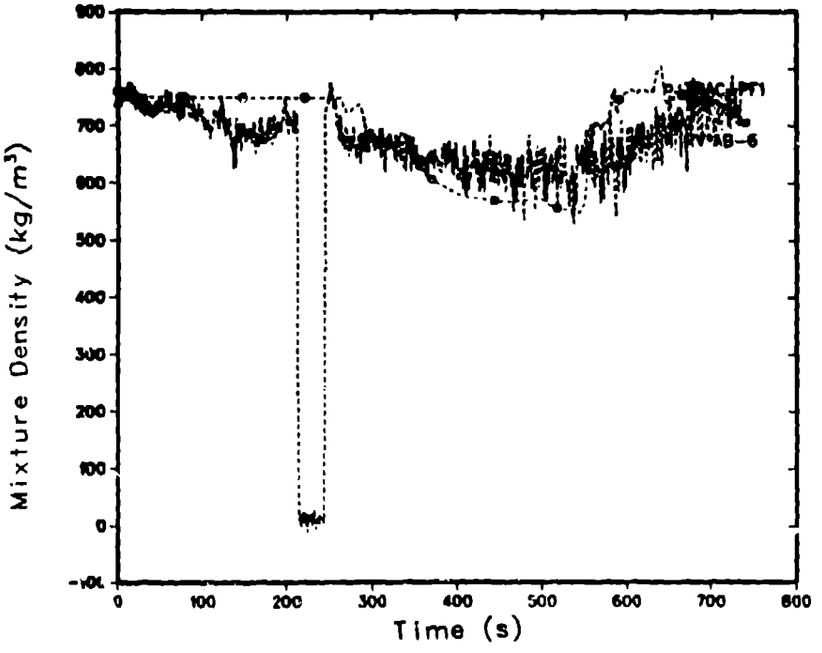

Fig. 4.
Comparison of the TRAC-calculated and measured fluid densities below the core for Semiscale Test S-UT-8.

the intact-loop seal provides the liquid inventory to drive the rapid and large increase in core inventory. Then, a slow boil-off of core inventory occurs until liquid from the accumulators arrives. As the test ends, the code is calculating the correct magnitude and trend in the core level.

Figures 5-7 compare cladding temperatures at three core elevations. At the 1.37-m elevation, the code calculates both dryouts to occur late and underpredicts the magnitude of the temperature excursions; these discrepancies, in light of the approximately correct core-level calculation (this elevation is well above the two minimums in the core level shown in Fig. 2), indicate that the code distributes the liquid inventory over too much height during the time the dryouts occur. At the 2.08-m elevation, the comparison is improved and the code overpredicts the magnitude of the temperature excursion following the second dryout. At the 3.55-m elevation, near the top of the core, the comparison is excellent although the code predicts that the final quenching process proceeds too rapidly. (It is interesting to note that at this elevation, the data do not show any effect of the early core-level depression even though the measured core liquid level goes to zero.)

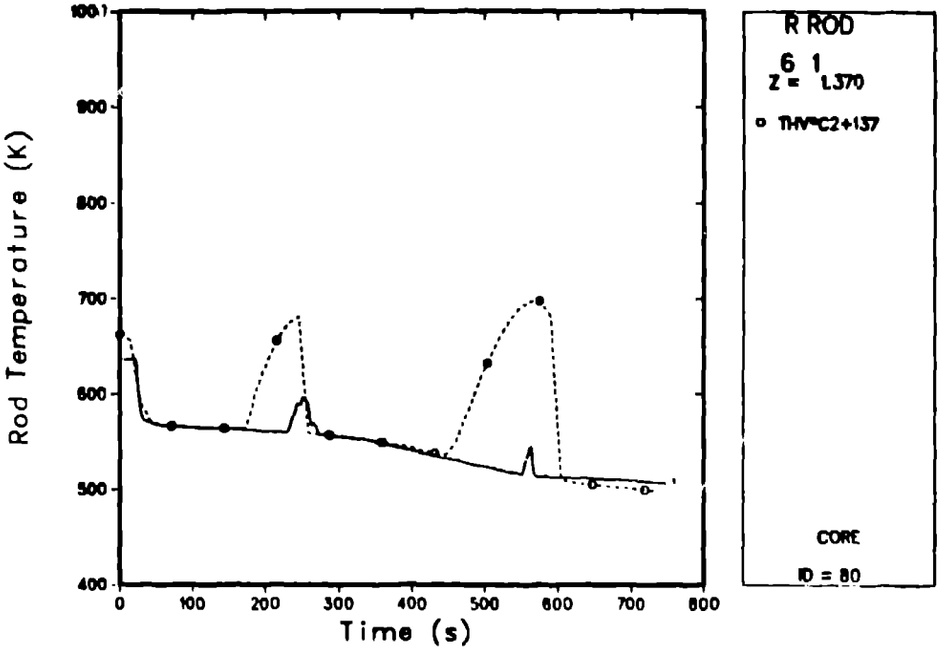

Fig. 5.
Comparison of the TRAC-calculated and measured cladding temperatures at the 1.37-m elevation for Semiscale Test S-UT-8.

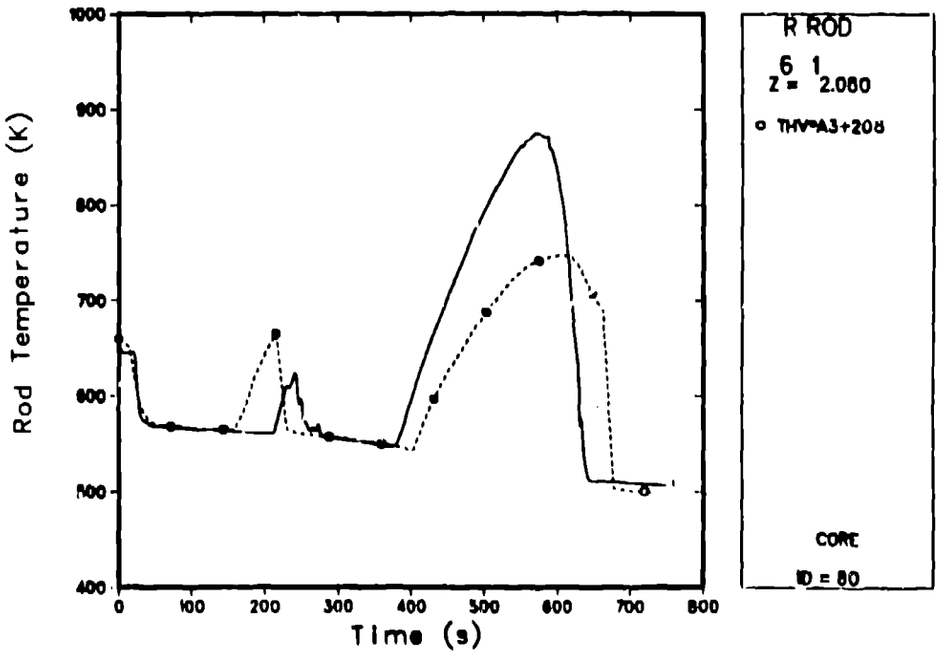

Fig. 6.
Comparison of the TRAC-calculated and measured cladding temperatures at the 2.08-m elevation for Semiscale Test S-UT-8.

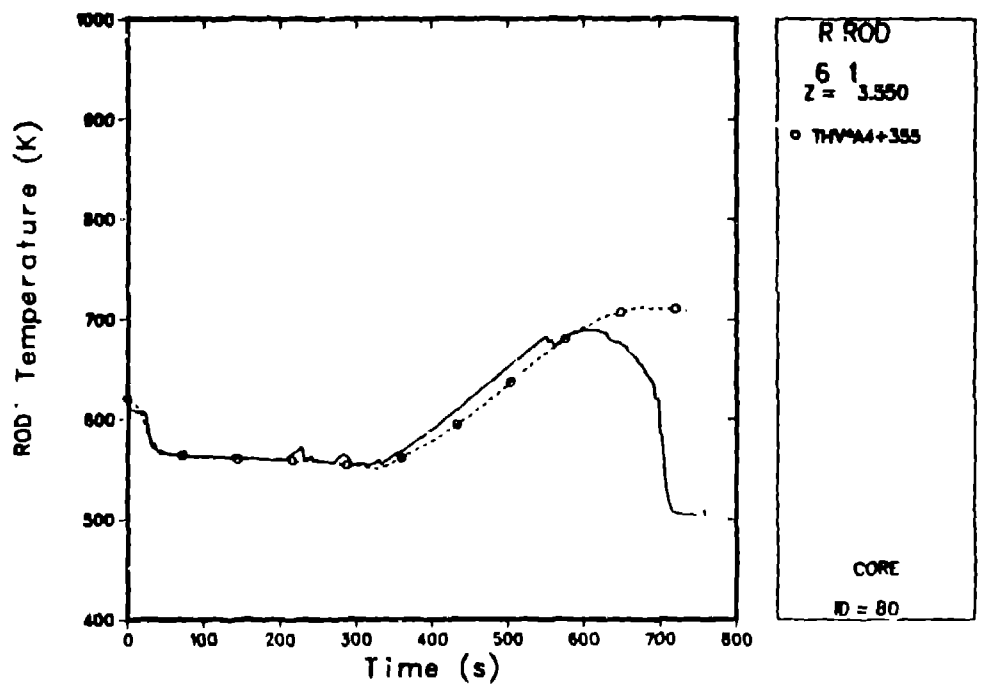

Fig. 7.
Comparison of the TRAC-calculated and measured cladding temperatures at the 3.55-m elevation for Semiscale Test S-UT-8.

Figure 8 shows the calculated and measured liquid levels in the intact-loop steam-generator tubes. The upside of the tubes is connected to the steam-generator inlet plenum, and the downside of the tubes is connected to the outlet plenum. The data for the first 100 s are influenced strongly by flow effects and should be ignored. The code calculates the correct, at least qualitatively, level formation and disappearance in the tubes, and its predictions are in good agreement with the data quantitatively. The differences in the upside and downside levels during the first 250 s drive the core levels below the minimum elevation in the pump-suction piping. The code calculates a similar behavior in the broken-loop steam generator. A sensitivity calculation in which we increased the steam-generator secondary noding adjacent to the tubes by a factor of two (halved cell sizes) shows that the TRAC-PF1/MOD1 calculated levels before ~250 s are insensitive to the change and that the core liquid level during this time is relatively unchanged. After ~250 s, the levels in the sensitivity calculation do change slightly, and the core-level increase after the initial minimum is reduced.

Figure 9 shows the central-processor-unit (CPU) time on a Cray-1S computer as a function of transient time. On average, this calculation required ~6 s of CPU time for each transient second.

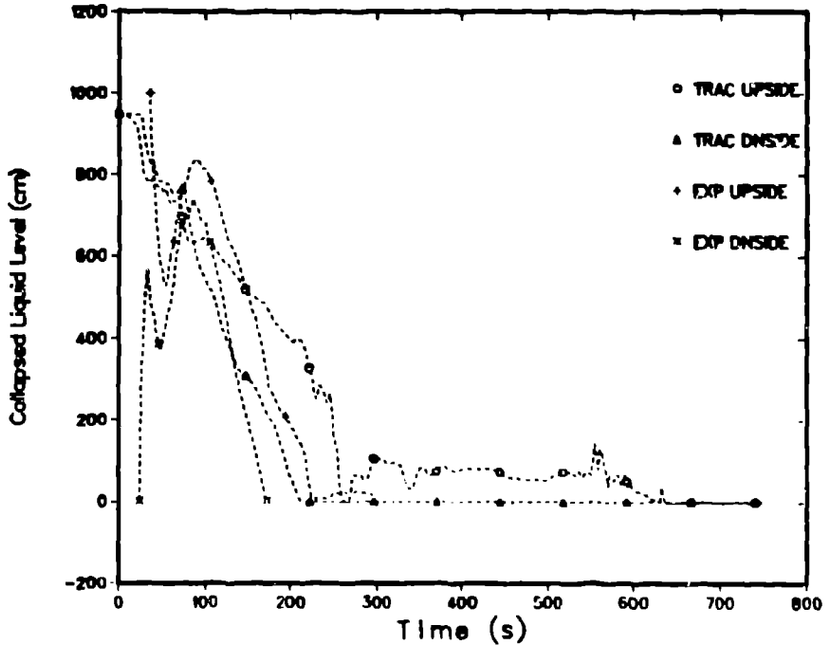

Fig. 8.
Comparison of the TRAC-calculated and measured intact-loop steam-generator-primary collapsed liquid levels for Semiscale Test S-UT-8.

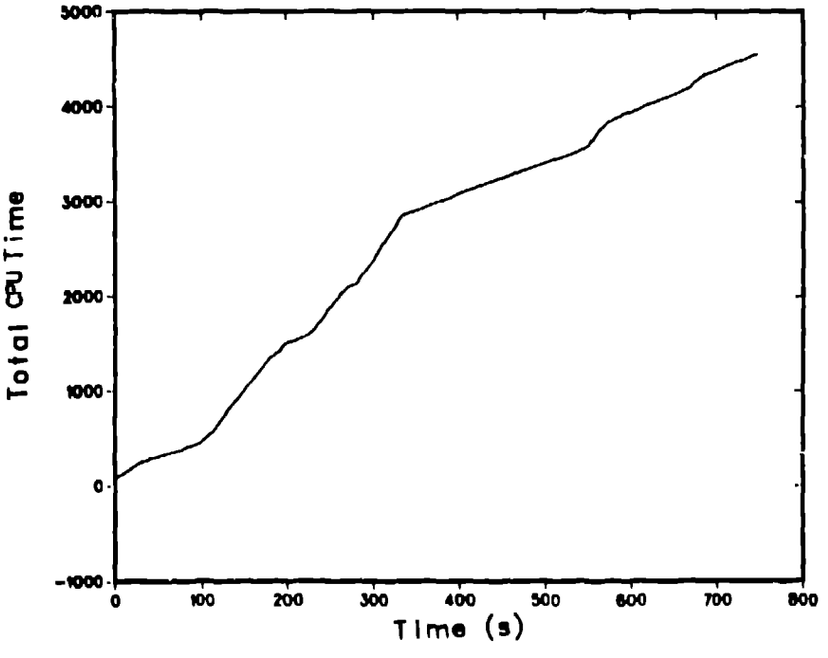

Fig. 9.
CPU time required for the Semiscale Test S-UT-8 transient analysis.

We tested the reactor kinetics and the hydraulics in TRAC-PF1/MOD1 by analyzing LOFT L9-4 (Ref. 13), an anticipated transient without scram (ATWS). This test is initiated by tripping the primary-coolant pumps and the main-feedwater pump and by closing the main steam-flow control valve. We discovered several errors in the programming of the reactor-kinetics models and in the reactivity feedback that provided the impetus to add a time-step control and time-step backup (repeat) based on the kinetics calculation. With these corrections and changes, the TRAC-PF1/MOD1 code correctly calculates the course of the L9-4 transient until the reactor scram occurs. We used the one-dimensional hydraulic modeling to obtain increased calculational speed. The input model consists of 39 TRAC components subdivided into 161 hydraulic cells.

Figure 10 shows the calculated and measured pressurizer pressures. This figure, as well as the remaining figures in this paper, shows a portion of the steady-state calculation (and data as appropriate). Following the initiation of the transient, the pressure rises until the safety-relief valve (SRV) begins to open and close cyclically to control the pressure. In the data, the SRV stops cycling at ~580 s, but the calculated SRV behavior continues to cycle until ~663 s. After the SRV stops cycling, the divergence in the measured and calculated pressures may be caused by small differences in the heating and cooling of the primary liquid and to leakage through the SRV.

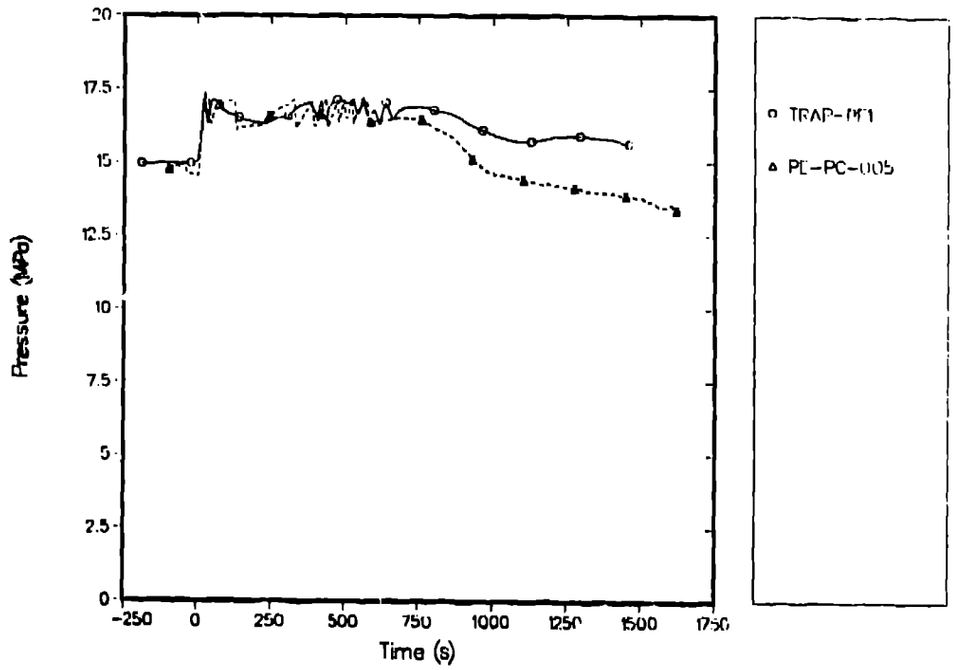

Fig. 10.
Comparison of the TRAC-calculated and measured pressurizer pressures for LOFT L9-4.

Figures 11 and 12 compare the measured and calculated liquid temperatures in the intact-loop hot and cold legs, respectively. Although there is some variation among the fluid-temperature measurements in the upper plenum, in the intact-loop hot leg, and in the steam-generator inlet plenum, Fig. 11 does show that the calculated temperature in the intact-loop hot leg is underpredicted following the initial rise after the beginning of the transient. Together, Figs. 11 and 12 indicate that the temperature rise across the core may be low during the first ~600 s. The temperature rise in the intact-loop cold leg that begins at ~250 s is caused by the degradation of the steam-generator-secondary heat transfer as the secondary liquid inventory is depleted. A corresponding rise in the intact-loop hot leg is not observed because the increased fluid temperature in the core reduces the core power.

Figure 13 shows the calculated and measured liquid velocities in the intact-loop hot leg. We adjusted the scale on this figure to show the detailed comparison after the pump trip. The calculated result lies within the indicated data uncertainty throughout the transient, although after ~800 s the calculation is near the upper extreme of the data uncertainty. Figures 14 and 15 show the calculated and measured primary-coolant pump speeds during the transient. The code correctly calculates the prolonged coastdown of pump number 1 and the rapid coastdown of pump number 2. The differences in the pump speeds reflect differences in the geometry and the hydraulic resistance associated with the flow paths through the two pumps.

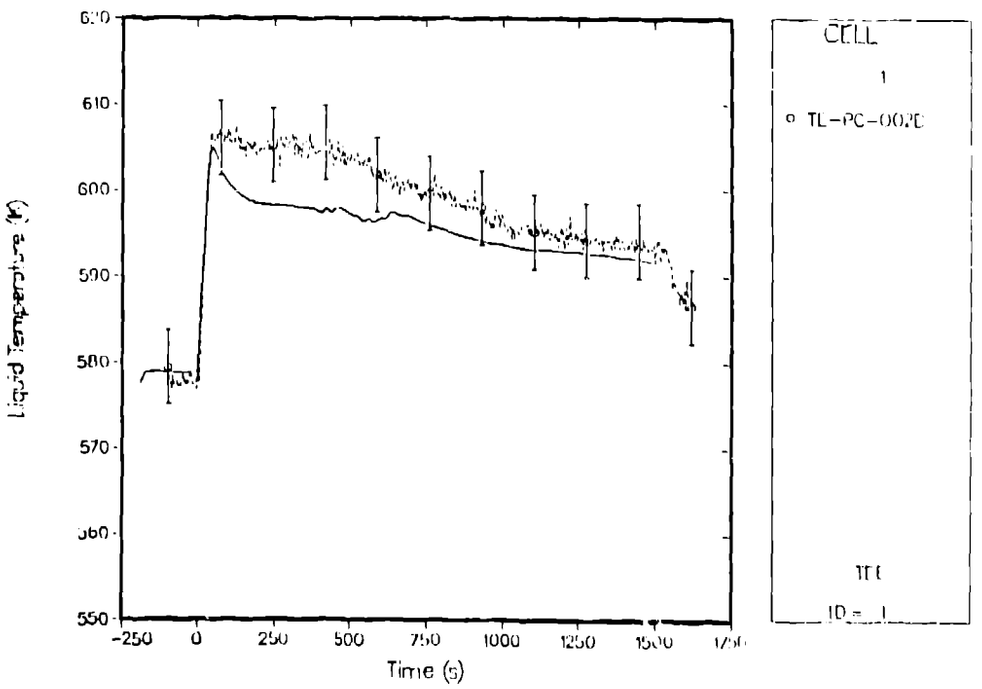

Fig. 11.
Comparison of the TRAC-calculated and measured intact-loop hot-leg liquid temperatures for LOFT L9-4.

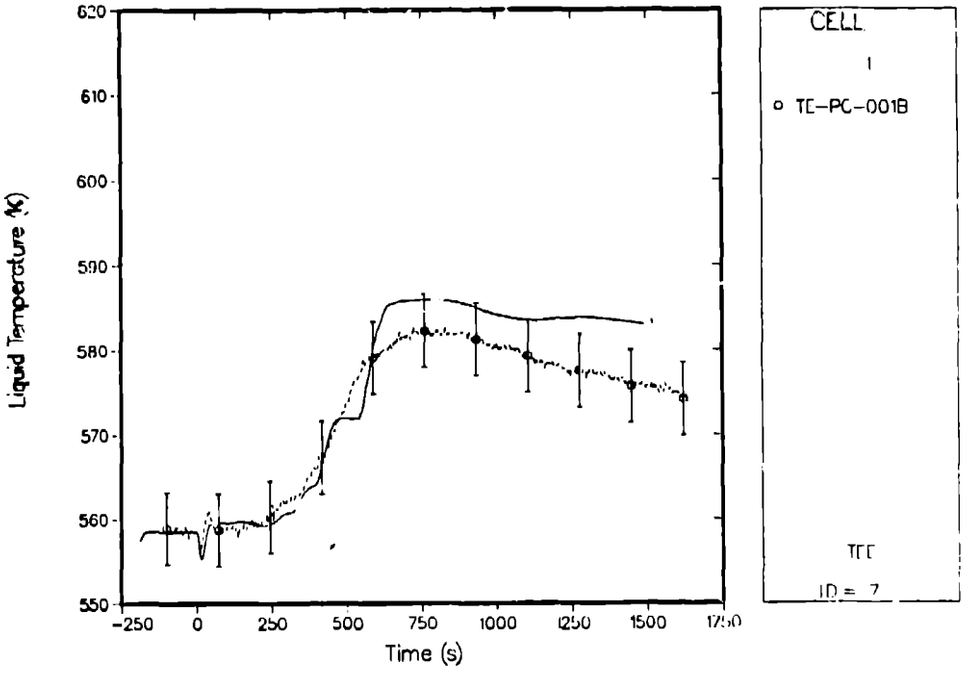

Fig. 12.
Comparison of the TRAC-calculated and measured intact-loop cold-leg liquid temperatures for LOFT L9-4.

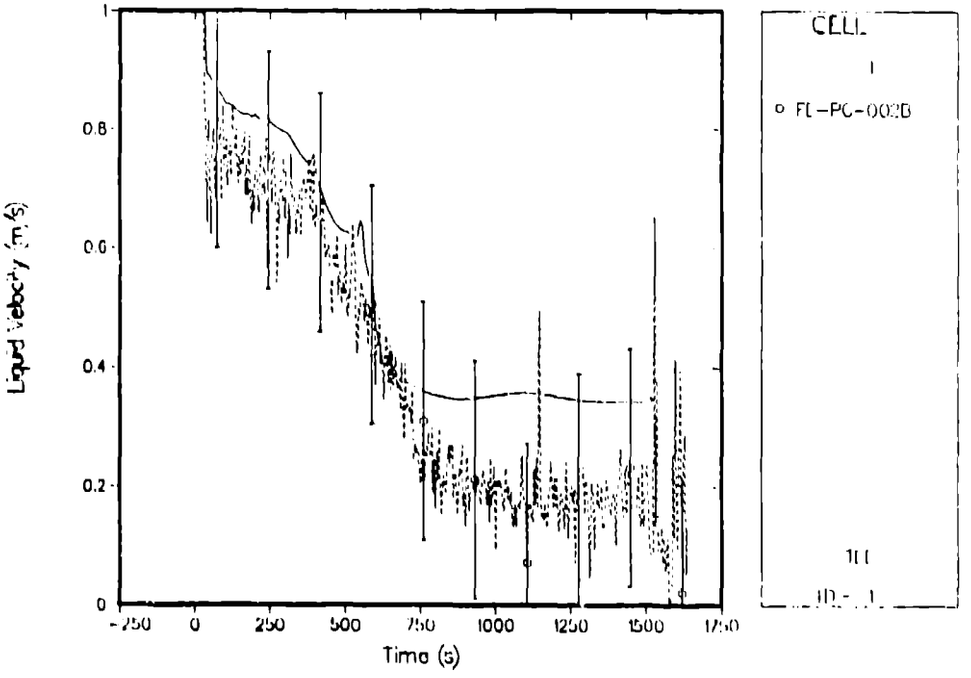

Fig. 13.
Comparison of the TRAC-calculated and measured intact-loop hot-leg liquid velocities for LOFT L9-4.

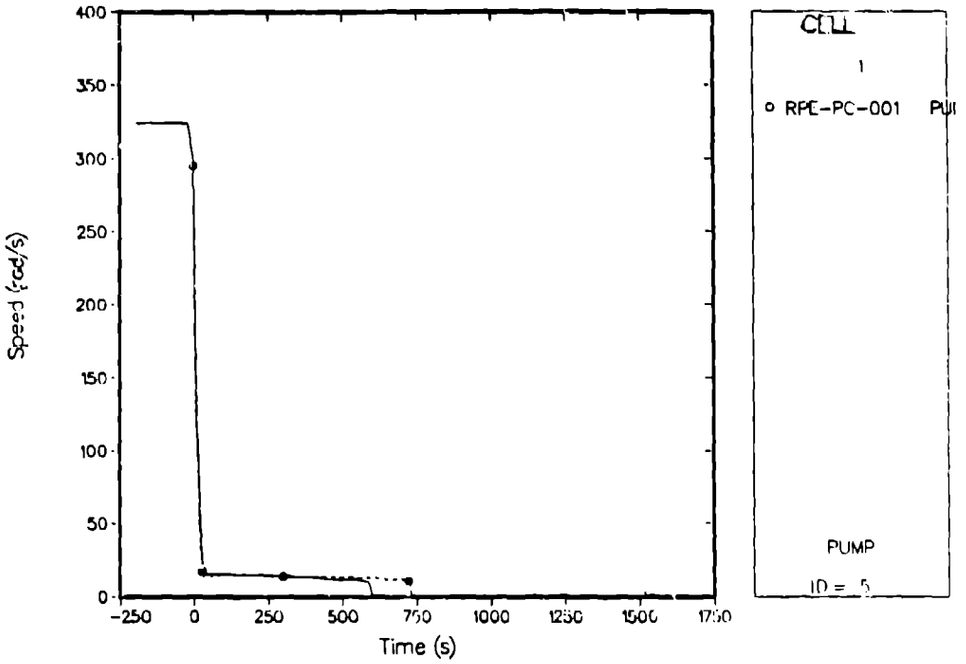

Fig. 14.
Comparison of the TRAC-calculated and measured primary-coolant pump speeds for pump number 1 for LOFT L9-4.

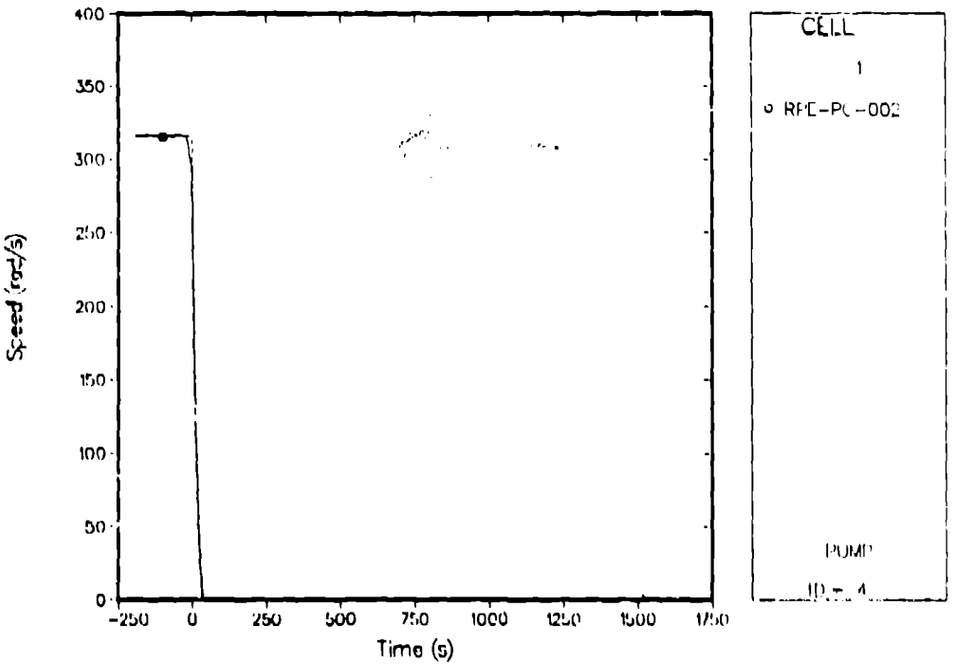

Fig. 15.
Comparison of the TRAC-calculated and measured primary-coolant pump speeds for pump number 2 for LOFT L9-4.

Figures 16 and 17 compare the calculated steam flows from the steam-generator secondary with two different measurements, the main steam-line flow and the bypass-line flow, respectively. Because of the relatively complex and varying control of the steam-generator-secondary pressure, we specified the secondary pressure as a boundary condition; the secondary pressure rises as the main steam-line valve closes until the steam-generator bypass valve controls the pressure (manually controlled by the operator). Figures 16 and 17 show that the steam flow decreases rapidly as the main steam-line valve closes and then increases as the steam-bypass valve opens. The comparisons in both figures are excellent, but the more accurate bypass-line measurement suggests that the steam flow between ~50 and ~100 s is slightly high.

Figure 18 shows the calculated and measured core powers. Again, we adjusted the scale of this figure to show more detail in the comparison. The comparisons in Figs. 10-18 are very good with the calculation generally lying within or near the data uncertainties; the major discrepancies occur in the broken-loop hot and cold legs and reflect a large uncertainty in the leakage through the reflood-assist bypass valves connecting the two piping legs and possibly the lack of a model to represent the thermal stratification of hot and cold liquid. The variations between the calculated curves and the data traces in Figs. 10-18, although small, are consistent and point to very small errors in the analysis.

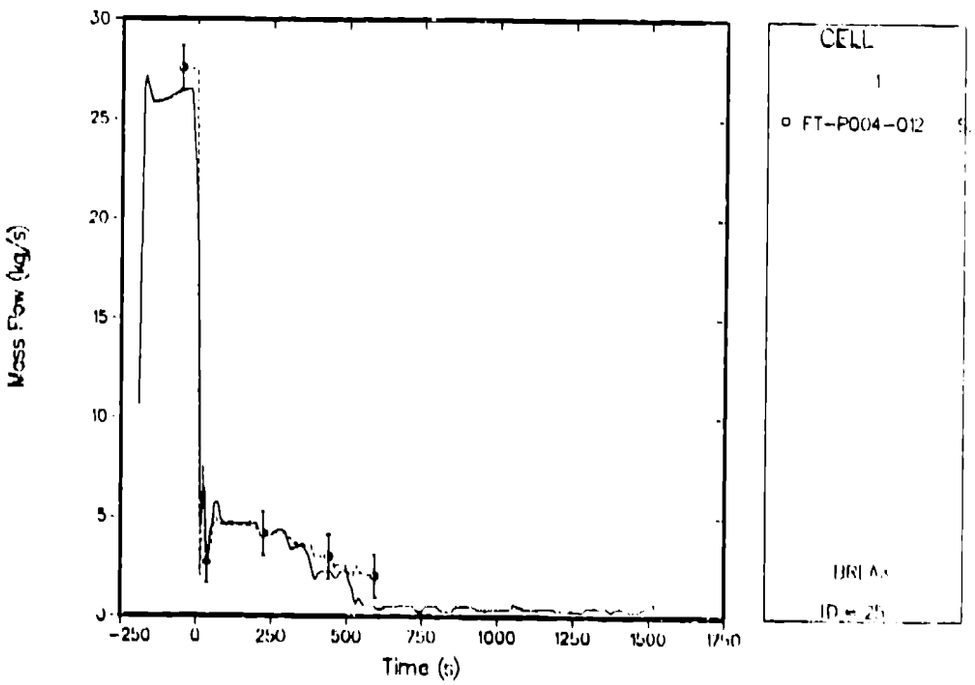

Fig. 16.
Comparison of the TRAC-calculated and measured steam-generator-secondary steam flows (with the main steam-line flow data) for LOFT L9-4.

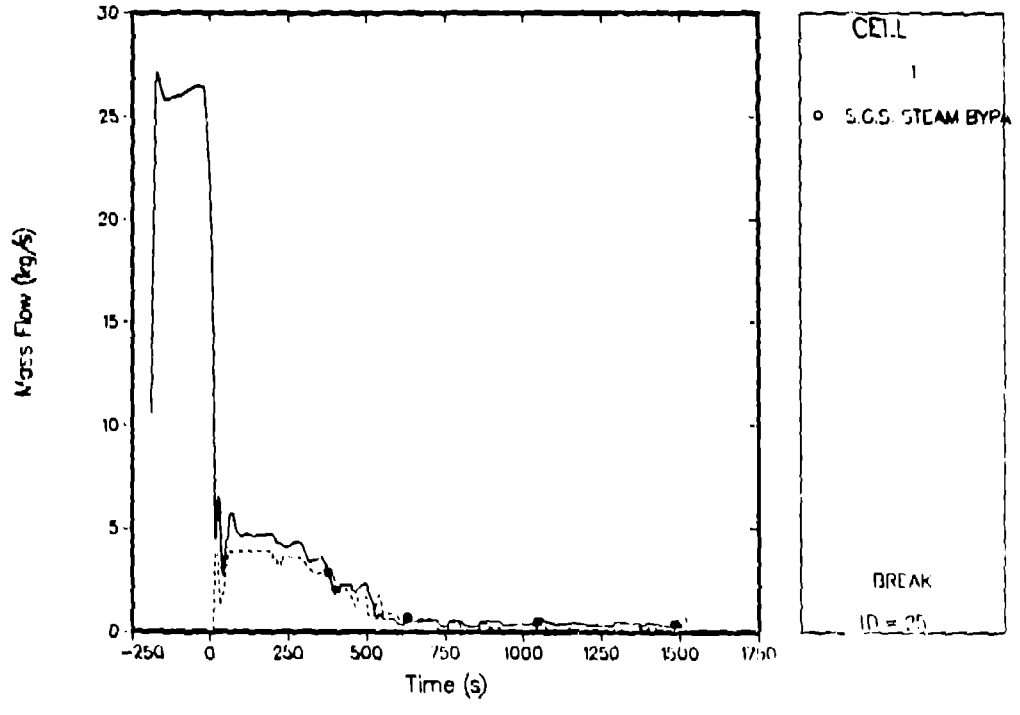

Fig. 17.
Comparison of the TRAC-calculated and measured steam-generator-secondary steam flows (with the steam-bypass flow data) for LOFT L9-4.

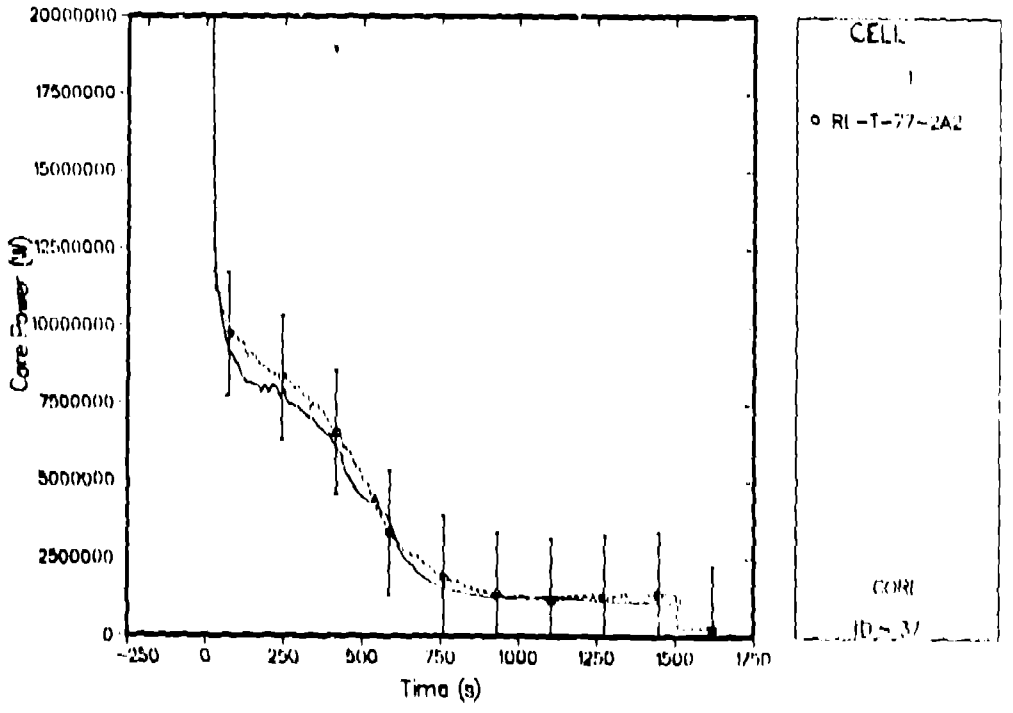

Fig. 18.
Comparison of the TRAC-calculated and measured core powers for LOFT L9-4.

Figures 19-22 summarize the reactor-kinetics calculation during the transient. The fuel-temperature reactivity (Fig. 19) becomes positive as the transient begins and remains positive throughout the transient because the fuel temperature drops and the reactor power decreases. The coolant-temperature reactivity in Fig. 20 becomes negative as the transient begins because the average coolant-temperature in the core increases after the primary-coolant pumps trip and the main steam-line valve closes; this figures reflects the changes in the intact-loop hot- and cold-leg liquid temperatures in Figs. 11 and 12. Because there is no core voiding, the void-fraction reactivity is not modeled. The programmed reactivity in Fig. 21 is used to account for the increased concentration of xenon as the power decreased; without this slight negative reactivity, the calculated core power late in the transient exceeded the data. These various contributions to the total reactivity combine to influence the reactor multiplication constant k (Fig. 22). The changes in the reactor multiplication constant directly affect the core power (Fig. 18). As expected, whenever the reactor multiplication constant approaches one, the calculated power tends to become constant.

Figures 23 and 24 show the CPU time on a Cray-1S computer and the time-step size as functions of the transient time.

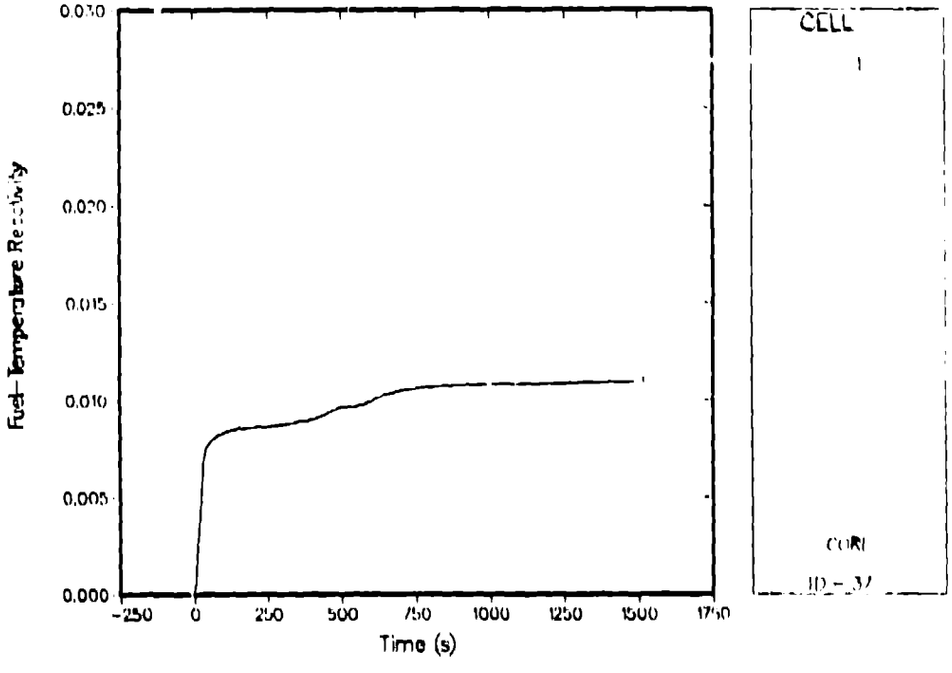

Fig. 19.
Calculated fuel-temperature reactivity for LOFT L9-4.

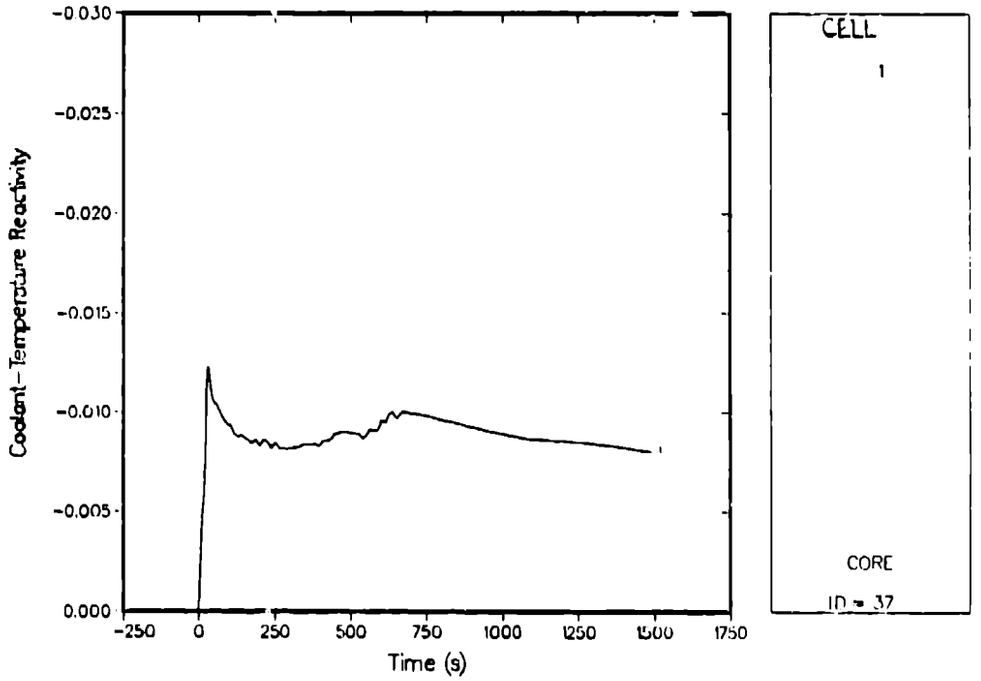

Fig. 20.
Calculated primary-temperature reactivity for LOFT L9-4.

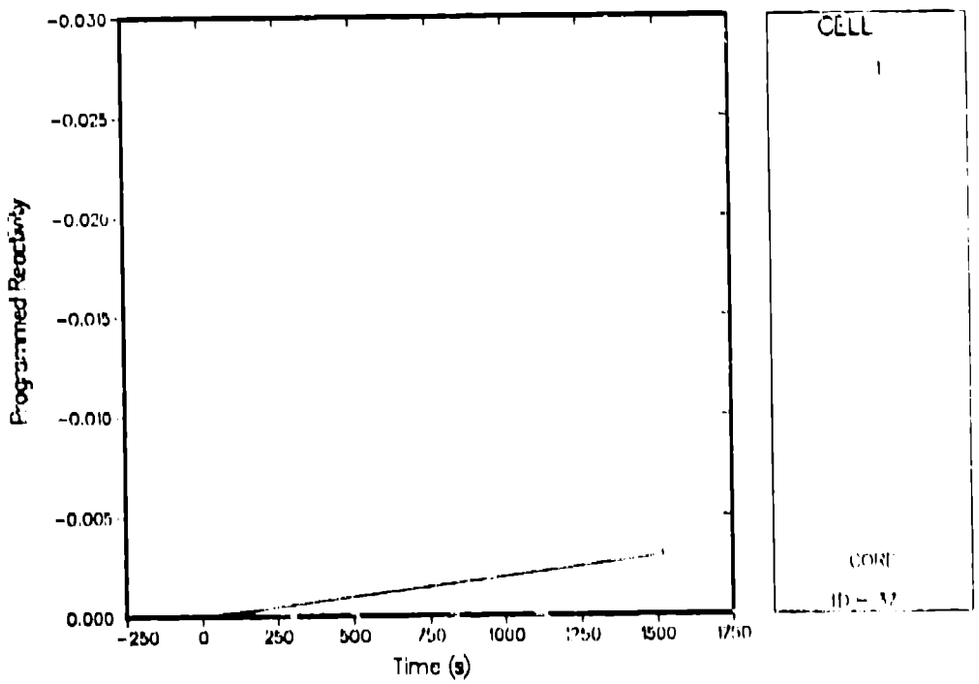

Fig. 21.
Programmed reactivity representing xenon poisoning for LOFT L9-4.

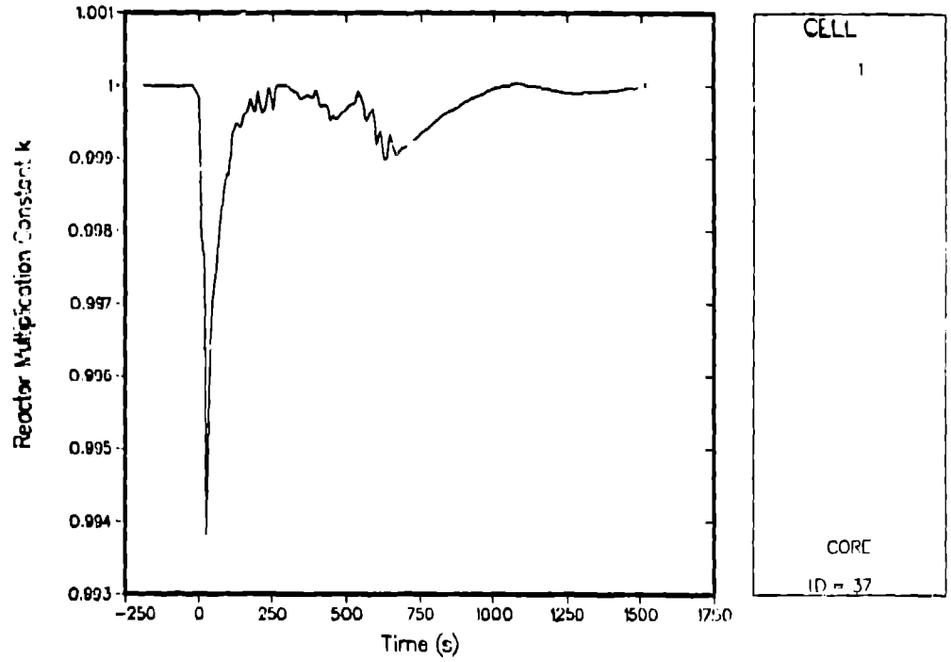

Fig. 22.
Calculated reactor multiplication constant k for LOFT L9-4.

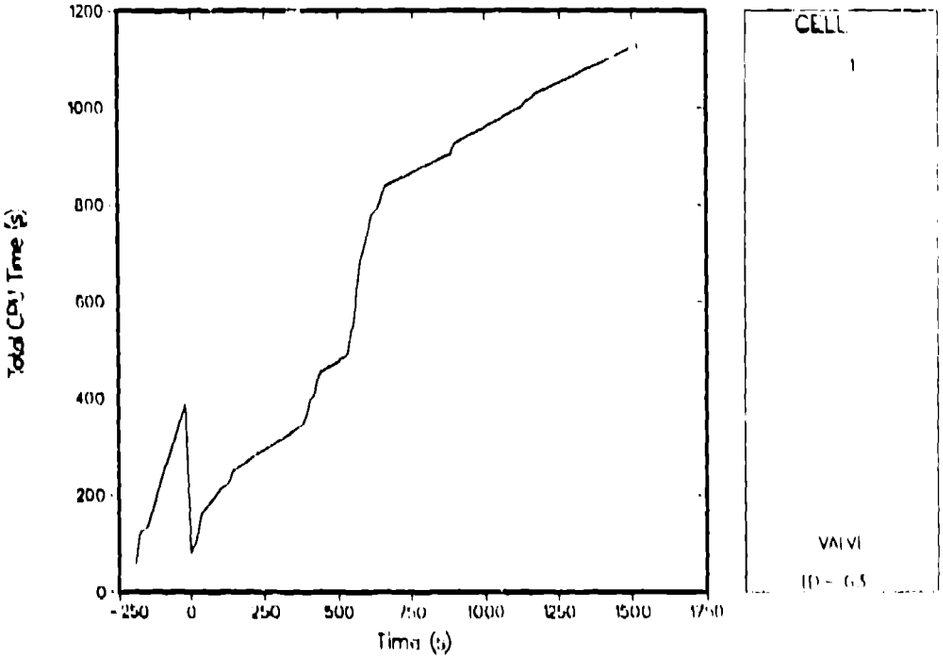

Fig. 23.
CPU time required for the LOFT L9-4 analysis.

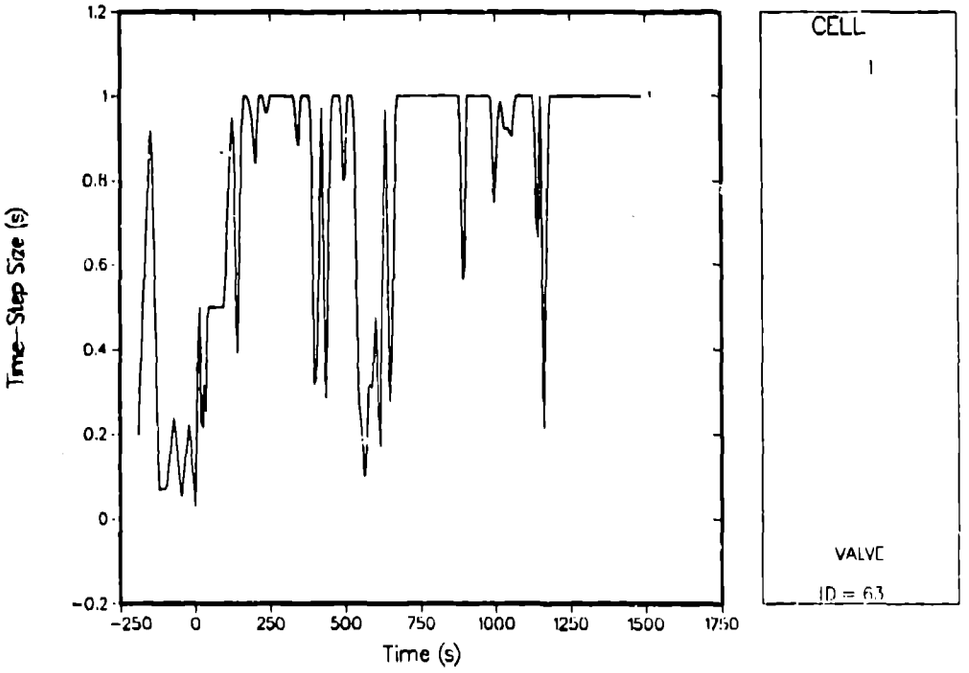

Fig. 24.
Time-step size used for the LOFT L9-4 analysis.

We currently are analyzing Semiscale tests from the steam-line and feed-line rupture test series to benchmark that capability in the code. These tests show the effects on the primary system of a severe transient in the secondary system and represent a rigorous test of the steam-generator modeling; the hydraulics to calculate level swell, phase separation, and liquid holdup; and the heat transfer.

In the past, we have analyzed LOFT large-break LOCAs L2-3, L2-5, and LP-02-6 with the TRAC-PD2 code. The LOFT Consortium conducted the LOFT LP-02-6 transient to represent the double-ended offset shear of the cold-leg piping from a condition of maximum power with an early pump trip. Our TRAC-PD2/MOD1 analyses of this test indicated that the code could calculate correctly the hydraulic phenomena early in the transient, but that the heat-transfer correlations prevented the calculation of the early core rewet and distorted the remainder of the transient. We are calculating this transient with the TRAC-PF1/MOD1 code to benchmark the large-break LOCA capability against the TRAC-PD2/MOD1 results. We also are using the reactor kinetics to calculate the core power instead of specifying the decay power as a function of time as in the TRAC-PD2/MOD1 calculation. The LOFT large-break LOCAs indicate that the final quenching of the core occurs shortly after the accumulator empties; however, the TRAC-PD2/MOD1 analyses show a later quenching. We have attributed at least part of this difference to the inability of previous code versions to inject the nitrogen from the accumulator as it empties and to force the final reflood of the core. Because

the TRAC-PF1/MOD1 code contains an air field, we are modeling the nitrogen injection in our TRAC-PF1/MOD1 analysis.

In conclusion, the TRAC-PF1/MOD1 analyses of Semiscale Test S-UT-8 compares very well with the data in general, and the code calculates all of the phenomena driving the depletion of core inventory during the transient. However, some of the differences observed in the comparison support the addition of a TRAC plenum component to represent in a straightforward manner multiple connections to a single cell and to avoid complex modeling with tee components. The LOFT L9-4 analyses have led to the correction of several errors in the reactor kinetics and subsequently demonstrated that capability.

The Los Alamos assessment effort indicates that the quality of the code improves as new code versions are released. And, although the work continues to indicate needed improvements in the code, the TRAC series of codes and specifically TRAC-PF1/MOD1 currently provide a very flexible tool for analyzing a wide variety of transients pertinent to PWRs.

REFERENCES

1. "TRAC-P1A: An Advanced Best-Estimate Computer Program for PWR LOCA Analysis," Los Alamos National Laboratory report LA-7777-MS, NUREG/CR-0665 (May 1979).

2. "TRAC-PD2: An Advanced Best-Estimate Computer Program for Pressurized Water Reactor Loss-of-Coolant Accident Analysis," Los Alamos National Laboratory report LA-8709-MS, NUREG/CR-2054 (April 1981).

3. "TRAC-PF1: An Advanced Best-Estimate Computer Program for Pressurized Water Reactor Analysis," Los Alamos National Laboratory report LA-9944-MS, NUREG/CR-3567 (February 1984).

4. "TRAC-PF1/MOD1: An Advanced Best-Estimate Computer Program for Pressurized Water Reactor Thermal-Hydraulic Analysis," Los Alamos National Laboratory report LA-10157-MS, NUREG/CR-3858 (to be published).

5. J. C. Vigil and K. A. Williams, "TRAC-P1A Developmental Assessment," Los Alamos National Laboratory report LA-8056-MS, NUREG/CR-1059 (October 1979).

6. Thad D. Knight and Vera B. Metzger, "TRAC-PD2 Developmental Assessment," Los Alamos National Laboratory report LA-9700-MS, NUREG/CR-3208 (to be published).

7. B. E. Boyack, "TRAC-PF1 Developmental Assessment," Los Alamos National Laboratory report LA-9704-MS, NUREG/CR-3280 (July 1983).

8. P. S. Saholta and F. L. Addessio, "TRAC-PF1/MOD1 Developmental Assessment," Los Alamos National Laboratory report (to be published).

9. T. D. Knight, "TRAC-P1A Independent Assessment - 1979," Los Alamos National Laboratory report LA-8477-MS, NUREG/CR-1652 (January 1981).

10. Thad D. Knight, "TRAC-PD2 Independent Assessment," Los Alamos National Laboratory report LA-10166-MS, NUREG/CR-3866 (to be published).

11. C. P. Booker, B. E. Boyack, P. Coddington, T. D. Knight, J. K. Meier, and J. R. White, "TRAC-PF1 Independent Assessment," Los Alamos National Laboratory report (to be published).

12. Robert K. Fujita, "TRAC-PF1/MOD1 Posttest Analysis of Semiscale Small-Break Test S-UT-8," Los Alamos National Laboratory report LA-UR-84-2079 (May 1984).

13. John K. Meier, "TRAC-PF1/MOD1 Posttest Analysis of LOFT L9-4, an Anticipated Transient without Scram," Los Alamos National Laboratory report (to be published).